Reactivated spatial context guides episodic recall

Nora A. Herweg[1], Ashwini D. Sharan[2], Michael R. Sperling[3], Armin Brandt[4], Andreas Schulze-Bonhage[4], Michael J. Kahana[1]

[1] Computational Memory Lab, Department of Psychology, University of Pennsylvania, Philadelphia, PA, USA
[2] Neurosurgery, Thomas Jefferson University Hospital, Philadelphia, PA, USA
[3] Neurology, Thomas Jefferson University, Philadelphia, PA, USA
[4] Epilepsy Center, University Medical Center, Freiburg, Germany
Correspondence: Dr. Nora A Herweg, nherweg@sas.upenn.edu or Dr. Michael J Kahana, kahana@sas.upenn.edu

Keywords: spatial memory; reinstatement; theta; gamma; hippocampus; parahippocampal gyrus; MTL; intracranial

Abstract

The medial temporal lobe (MTL) is known as the locus of spatial coding and episodic memory, but the interaction between these cognitive domains, as well as the extent to which they rely on common neurophysiological mechanisms is poorly understood. Here, we use a hybrid spatial-episodic memory task to determine how spatial information is dynamically reactivated in sub-regions of the MTL and how this reactivation guides recall of episodic information. Our results implicate theta oscillations across the MTL as a common neurophysiological substrate for spatial coding in navigation and episodic recall. We further show that spatial context information is initially retrieved in the hippocampus (HC) and subsequently emerges in the parahippocampal gyrus (PHG), which is known as the main input region to the HC during encoding. Our results therefore support the notion that the predominant direction of information flow in the MTL reverses during retrieval. Finally, we demonstrate that hippocampal theta phase modulates parahippocampal gamma amplitude, suggesting a role for cross frequency coupling in coding and transmitting retrieved information.

Introduction

Spatio-temporal context provides a unique tag for each event we experience, and the similarities among these contextual tags serve to organize the contents of episodic memory. This organization cannot be observed directly but can be inferred from the way people recall information. When remembering lists of words, people exhibit a robust tendency to successively recall words that occurred in neighboring list positions [1,2]. While most studies on episodic memory focused on this *temporal contiguity* effect, more recent research has shown that spatial context similarly guides recall transitions. During recall of items presented in a 3D virtual environment, participants showed a *spatial contiguity* effect, meaning that they recalled items in succession that were presented at proximate locations in the environment [3]. These results suggest that both temporal and spatial context are reactivated during recall and cue associated items. They further establish a direct link between spatial coding and episodic memory, two cognitive domains that have been associated with the medial temporal lobe (MTL) in parallel lines of research.

During navigation, single cells in the hippocampus (HC) and entorhinal cortex represent current spatial location with a single place field (i.e. place cells) [4,5] or multiple place fields arranged in a hexagonal grid (i.e. grid cells) [6,7], respectively. These firing patterns are accompanied by hippocampal low frequency oscillations in the delta to theta band which are prominent in raw traces and manifest in increased spectral power during movement compared to stillness [8–16]. In rodents a direct relationship between the two phenomena has been observed: Place cells fire at progressively earlier phases of the theta cycle, as a rat traverses a place field [17]. Moreover, grid cell firing can be silenced by inhibiting theta oscillations [18,19]. In humans, increased delta-theta power during navigation, immediately preceding navigation or during a cued location memory task has been linked to navigation performance [10,13] and spatial memory accuracy [16]. Together, these results suggest that low frequency oscillations orchestrate place and grid cell firing and are

part of a coding scheme for spatial information in the service of orientation and navigation [20].

In the episodic memory domain, the HC and surrounding parahippocampal gyrus (PHG), are known as the MTL memory system [21]: a system thought to form and retrieve event memories by associating arbitrary stimulus combinations. Across different theories, there is consensus that the PHG (including perirhinal, parahippocampal and entorhinal cortices) processes memory attributes earlier and more distinctly than the HC [22–25]. Accordingly, item and spatio-temporal context information are assumed to be represented mostly separately in the PHG [23,24]. The PHG projects to the HC, where item information is integrated with spatio-temporal context information [22–25]. Despite the striking anatomical overlap of spatial coding and episodic memory in the MTL, remarkably little is known about potential shared neurophysiological mechanisms. Theta oscillations have been suggested to support the formation of both spatial and episodic associations by organizing spike-timing and associated plasticity [26], but evidence in favor of this idea is scarce. In fact, successful episodic memory operations are often associated with a wide-spread decrease in low- and increase in high-frequency power [27,28]. Despite such broad-band tilt effects, however, there also seem to be more localized increases in temporal narrow-band theta oscillations during successful encoding [29] and retrieval [28], which might more specifically be linked to recollection of contextual information [30,31].

Here, we use a hybrid spatial-episodic memory task in combination with intracranial electroencephalography (iEEG) to assess the role of low- and high-frequency activity for episodic retrieval of spatial context information in the MTL. In our task, participants played the role of a courier, riding a bicycle and delivering parcels to stores located within a virtual town (**Figure 1a-b**). On each trial participants navigate to a series of stores and subsequently are asked to recall all objects they delivered. Based on the prominent role of theta oscillations for spatial memory and the idea that they specifically relate to contextual retrieval, we hypothesize that episodic retrieval of spatial context information, in contrast to more general biomarkers of successful memory, is accompanied by increased medial temporal theta power.

We then turn from spectral biomarkers of spatial context retrieval to more specific reactivated spatial representations. Prior research has shown that place-responsive cells throughout the human MTL that fire while a subject is navigating a certain part of a virtual environment, reinstate their activity during recall of words that were encoded in that part of the environment [32]. The temporal dynamics of reinstatement in different MTL sub-regions, however, remained unknown. To assess these dynamics, we use representational similarity analyses in combination with a sliding window approach.

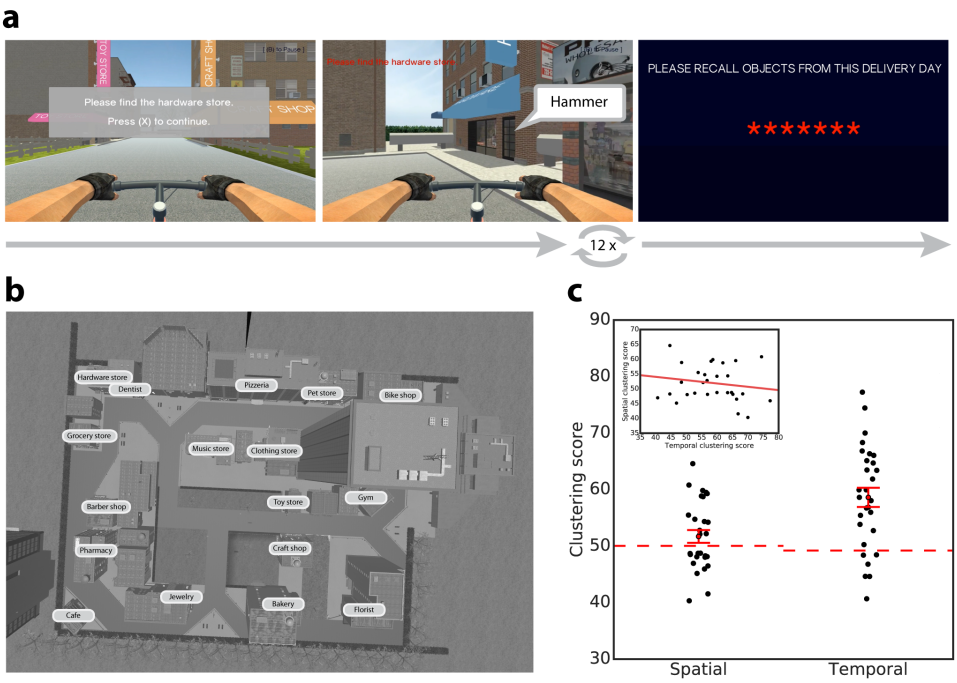

Figure 1. Task design and behavioral clustering. a) Hybrid spatial-episodic memory task in which participants play the role of a courier. On each trial, participants navigate to 12 different target stores to deliver parcels. Upon arrival at a target store, participants are presented with the object that they have just delivered. After 12 deliveries, participants navigate to a final store. Here, the screen goes black and participants are asked to freely recall all objects they delivered in any order. b) Bird's-eye view of the virtual city containing streets, target stores, non-target buildings and props such as fences and trees. Participants never get to see this view. c) Clustering in recall sequences. Participants organize their recalls with respect to spatial and temporal context information. Error bars show the standard error of the mean (SEM). Dashed red lines indicate the average of a permutation distribution. Spatial and temporal clustering are uncorrelated across subjects (inset).

Based on the idea that information flow in the MTL reverses during retrieval [33], we propose that spatial information is initially retrieved in the HC, and from there reinstates activity in PHG.

Finally, we ask how retrieved information is transferred between PHG and HC. Theta oscillations have been strongly implicated in inter-regional connectivity during successful memory operations [27,30,34] and in rodents place-responsive cells are locked to both theta and gamma oscillations [35,36]. Furthermore, cells with overlapping place fields may fire within the same gamma and theta cycle, suggesting that assemblies of neurons with similar tuning properties are organized by a theta-gamma code [37,38]. Based on these findings, we suggest that theta and gamma oscillations promote information transfer between HC and PHG during retrieval of episodic information encoded in a spatial environment [27,39]. Specifically, we explore whether theta phase to gamma amplitude coupling between HC and PHG increases during recall to facilitate information transfer from HC to PHG.

Results

Participants showed significant temporal ($p < 0.001$) and spatial ($p = 0.04$) clustering in their recall sequences (**Figure 1c**), meaning that they were more likely to recall items in succession, which were encoded at proximate serial positions or locations in the virtual environment. Across subjects there was no correlation between spatial and temporal clustering scores ($r = -0.15$, $p = 0.43$), suggesting that these phenomena occur independently and are not driven by a common variable like associative memory performance or strategy use.

To assess the role of theta and gamma activity in the HC and PHG for successful spatial context retrieval and associated spatial clustering, we used a within-subject linear regression model relating power preceding recall to the spatial proximity between successively recalled items. Assuming that retrieved spatial context serves as a cue for items encoded in close spatial proximity, the spatial proximity associated with a recall transition should be indicative of the degree of spatial context retrieval (**Figure 2a**). **Figure 2b** shows the β parameters for spatial proximity. We found a significant effect of frequency ($F_{(1,74)} = 5.57$, $p = 0.02$), with more positive β's for theta than high gamma power. Average β's in the HC and PHG were also significantly different from zero for theta ($t_{(24)} = 2.29$, $p = 0.03$) but not gamma ($t_{(24)} = 0.96$, $p = 0.35$) power. Positive parameters indicate

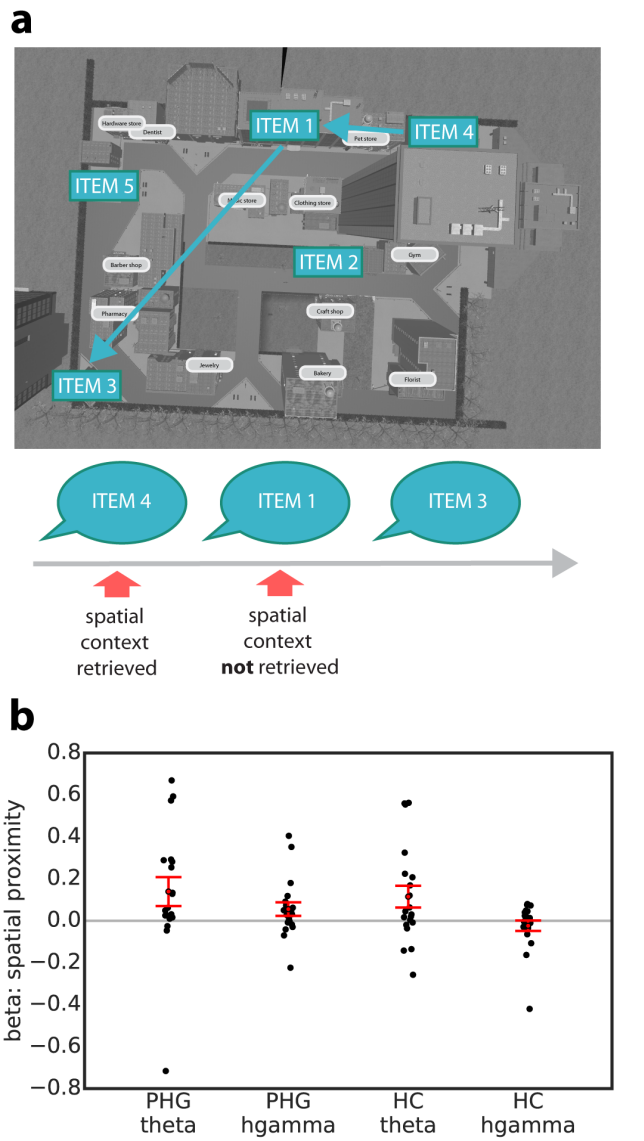

Figure 2. Spectral power during recall transitions as a function spatial proximity. a) Assuming that retrieved context cues items experienced in a similar context, the spatial proximity associated with each recall transition was used as a proxy for spatial context retrieval. b) ß parameters (± SEM) from our within-subject regression analysis relating spatial proximity to spectral power preceding recall. Theta, but not high gamma (hgamma), power increases in hippocampus (HC) and parahippocampal gyrus (PHG) during spatial context retrieval (i.e. for the first item in a spatially close recall transition).

increases in power during retrieval of spatial context (i.e. for the first item in a spatially close recall transition). There was no effect of brain region ($F_{(1,74)} = 1.18$, $p = 0.28$) and no interaction ($F_{(1,74)} = 0.34$, $p = 0.56$). These results suggest that retrieval of spatial information during episodic free recall and associated clustering of recall sequences is associated with increased theta power in the HC and PHG.

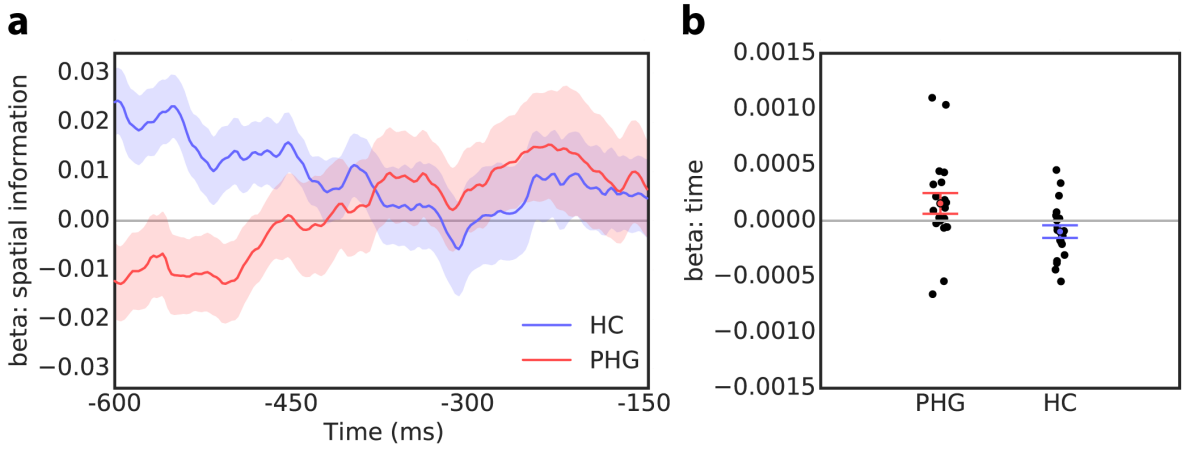

Figure 3. Reinstatement of spatial information leading up to recall. We used a within-subject regression model with a sliding-window approach to relate neural encoding-retrieval similarity to the spatial proximity between the locations associated with the respective encoding and recall events. a) Each data point reflects similarity as function of spatial proximity for a 300 ms encoding time window and a sliding 300 ms retrieval time window centered between -600 and -150 ms (i.e. half a window size from the edges of each retrieval epoch). A β above 0 indicates higher similarity for encoding-recall pairs that share spatial context and, hence, can be interpreted as reactivated spatial information. Spatial information is represented more strongly in hippocampus (HC) at the beginning of the epoch. Subsequently, information numerically decreases in HC and increases in PHG leading up to recall. Shaded error represents SEM. b) We quantified this temporal trend in both brain regions with within-subject linear regression. The resulting second order β parameters are displayed ± SEM. They are on average positive in PHG, negative in HC, and significantly higher in PHG than HC, confirming that these regions exhibit distinct temporal profiles of spatial context reinstatement.

Next, we sought to assess dynamic reinstatement of specific spatial representations in HC and PHG. To this end, we used encoding-retrieval similarity analyses with a sliding window approach. A vector representing power during encoding for all electrodes in HC or PHG, all frequencies and time-points was correlated with a corresponding retrieval vector derived from a sliding time-window to track reactivation (i.e. neural similarity) of encoding features leading up to recall. We then used a linear regression model relating neural similarity at each time point to the spatial proximity between the locations associated with the encoding and recall event. A β value above 0 indicates higher similarity for encoding-recall pairs that share spatial context and, hence, can be interpreted as reactivated spatial information. To exclude confounding this measure with reinstatement of item-level information, we excluded encoding-recall pairs of the same item. We observed distinct temporal profiles of spatial context reinstatement in the HC and PHG: Whereas our index of retrieved spatial information numerically decreased in the HC, it increased in the PHG leading up to recall (**Figure 3a**). The initial difference between HC and PHG was statistically significant ($t_{(38)} = 3.56$, $p = 0.001$), whereas there was no significant difference between PHG and HC at the end of the time series ($t_{(38)} = 0.15$, $p = 0.88$). We also assessed the difference in temporal trend using within-subject linear regression models within each region. The second order β parameters obtained from these models reflect the change in spatial information over time leading up to recall. They were on average positive in PHG (i.e. spatial information increased), negative in HC (i.e. spatial information decreased), and significantly different from each other ($t_{(38)} = 2.32$, $p = 0.03$; **Figure 3b**). These results support the notion that spatial information is initially retrieved in the HC and then relayed to cortical modules in the PHG.

Finally, we explored theta-gamma phase-amplitude coupling between these two brain regions (i.e. a modulation of parahippocampal gamma amplitude by hippocampal theta phase) as a mechanism of information transfer. To this end we calculated the synchronization index (SI) [40] between hippocampal theta phase and the phase of the parahippocampal gamma power envelope for all HC-PHG electrode pairs during recall. We observed significant phase-amplitude coupling (PAC), as determined by a non-parametric permutation procedure, in 11 out of 96 electrode pairs (11.5%; **Figure 4a-b**). PAC was significant at the subject level, when averaged over all electrode pairs per subject ($p = 0.003$), with an average phase offset of 9.0 ° (**Figure 4c**). However, PAC was not significantly correlated with spatial clustering ($r = -0.09$, $p = 0.75$) or

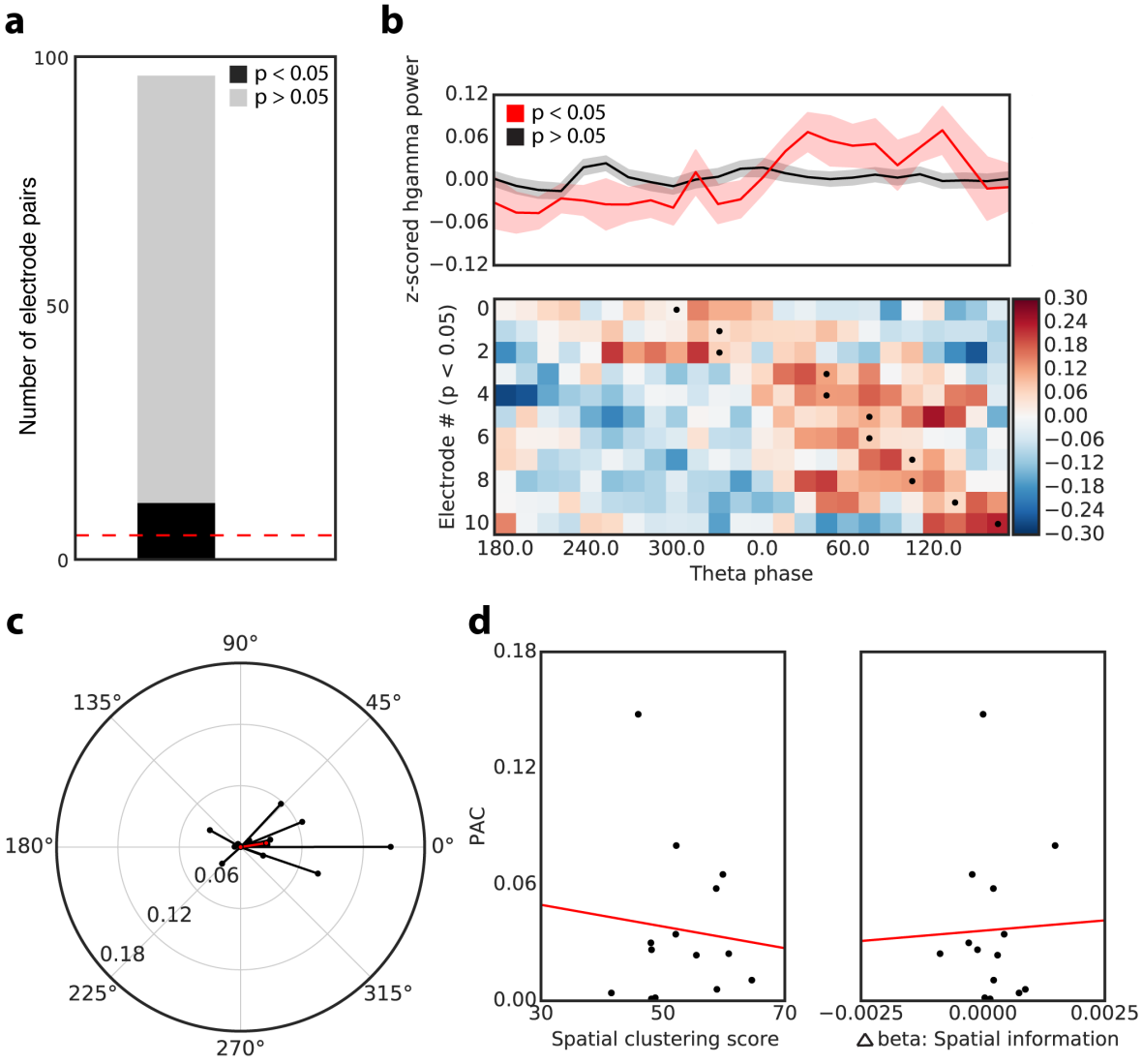

Figure 4. Theta phase to gamma amplitude coupling between hippocampus (HC) and parahippocampal gyrus (PHG). a) 11 out of 96 electrode pairs (11.5%) exhibited significant phase amplitude coupling (PAC). Red dashed line indicates 5% mark. b) z-scored high gamma power in PHG shown as a function of HC theta phase. Top panel shows average power (± SEM) for all significantly coupled electrode pairs in red and average power (± SEM) for all other electrodes in black. Lower panel shows z-scored power in individual significant electrode pairs. Electrode pairs are sorted by average phase offset for each pair, indicated by black dots. c) Average synchronization index (SI) per subject (black) and across all subjects (red). The length of each line reflects coupling strength and the orientations reflects phase offset. Coupling across subjects was significantly greater than chance as determined with a permutation test. d) PAC as a function of spatial clustering score (left; displayed in Figure 1c) and the difference in β parameters for the temporal trend of spatial information in PHG and HC (right; displayed in Figure 3b). We did not observe a significant relation between these variables.

spatial information transfer between PHG and HC ($r = 0.03$, $p = 0.92$; i.e. the difference in β parameters for the temporal trend of spatial information between PHG and HC) across subjects (**Figure 4d**). We therefore conclude that PAC between HC and PHG supports episodic recall, but cannot be specifically linked to inter-individual differences in retrieval of spatial context information.

Discussion

Episodic memory refers to our ability to associate events with a specific spatio-temporal context. Whereas numerous studies have long implicated temporal context as a powerful organizing principle in episodic retrieval [1,2], spatial context has only recently received attention [41,42]. Our behavioral results demonstrate that when a

spatial study context is made available by use of a virtual environment, participants are more likely to recall items in succession that were encoded at proximate spatial locations. This spatial contiguity effect mirrors the well-established temporal contiguity effect in which participants also tend to successively recall items studied in temporally proximate positions within a series. We thus find that like temporal context, spatial context also appears to reinstate during episodic memory retrieval.

To help elucidate the physiological basis of spatial-context reinstatement, we related the spatial proximity associated with each recall transition (a measure of spatial-context reinstatement) to spectral power during retrieval. We observed increased medial temporal theta, but not gamma power, to co-occur with retrieval of spatial context and associated clustering. This finding is of particular interest, given the known role of theta oscillations in navigation and spatial memory [20]. Theta oscillations have been observed in the rodent [8,9] and human [11,12,14,15] MTL during movement compared to stillness. In rodents, they have been linked to the spiking of place responsive cells [17–19]. In humans, theta power in the MTL has been implicated in coding spatial distances during and preceding navigation [12] or during teleportation [43], suggesting that spatial distances are coded in theta even in the absence of sensory cues. In a cued location memory task, theta power has further been shown to be indicative of successful encoding of spatial locations [16]. And using MEG, theta power has been related to cued retrieval of spatial locations and navigation performance [10,13]. Taken together these findings implicate theta in the encoding, retrieval and online-maintenance of spatial locations that underlie spatial orientation and navigation. Notably, in our task, the increase in theta power we observed occurred in the absence of any affordances to maintain or recall spatial information, while participants viewed a black screen. Our results therefore extend previous findings to suggest that theta oscillations provide a common electrophysiological signature of spatial coding during navigation, explicit spatial memory demands and incidental episodic retrieval of spatial context information.

But where, when and how exactly is spatial information retrieved? It has previously been shown that place-responsive cells in the human MTL reinstate their spiking activity during recall of items encoded within a cell's place field [32]. It remained unknown, however, what the temporal dynamics of reinstatement in different MTL sub-regions are and how information is routed between them. The results of our encoding-retrieval similarity analysis suggest that spatial information is reinstated with distinct temporal profiles in HC and PHG. Whereas spatial information is reinstated early in HC, information in PHG builds up closer to recall. This pattern of results suggests that initial retrieval of spatial information occurs in the HC and, from there, is relayed to the PHG. It thereby supports theories claiming a reversal of information flow between HC and neocortex during encoding and retrieval [33] and is in line with an fMRI study on cued recall of object-scene pairs: Staresina and colleagues (2013) observed differential onset latencies in category-selective regions of the PHG specialized for objects and scenes, depending on which type of information served as object and which as cue. Dynamic causal modeling analyses in the same data set favored a model in which information was routed from PHG via HC back to PHG [44]. Taken together, the locus of retrieval for associations between item and spatial context (or objects and scenes) seems to be the HC, from where information is relayed to cortical regions in the PHG that provided input to the HC during encoding.

Our results, however, do not reveal what kind of representation is reinstated in HC or PHG. Spatially responsive cells have different tuning properties in different sub-regions of the MTL. In the rat, place cells with the most distinct firing fields are found in the CA areas of the HC, whereas grid cells are found in the entorhinal cortex [45]. Evidence in humans is scarce but seems to be broadly consistent with this [4,6,46]. In humans, a different type of cells located in the PHG responds to view of specific landmarks, irrespective of a subjects' location [4], suggesting that these cells are more sensitive to visual features than abstract location. Based on these and other considerations [23,24], one can expect that the type of spatial representation that is reinstated, as well as its link to other types of episodic content, differs between different regions in the MTL, potentially with an abstract to concrete gradient from HC, over entorhinal cortex, to PHG. Whereas our analyses of spatial context reinstatement assumed a linear relation between actual and representation spatial distance (i.e. **Figure 3** shows the linear relation between neural similarity and spatial proximity over time), it is possible that some regions of the MTL do not represent spatial information on such a linear scale: A region that primarily cares about visual features of scenes, for instance, might exhibit strong neural similarity at all locations providing a similar view and low similarity otherwise.

Our connectivity analyses revealed significantly greater than chance theta-phase to gamma-amplitude coupling between HC and PHG during recall. Prior studies in humans have implicated local theta-gamma coupling within the HC as well as coupling between frontal and posterior regions in scalp EEG to successful memory encoding [47–49]. In rats, coupling in CA regions of the HC was associated with successful retrieval [50,51]. Our results demonstrate, that theta-gamma coupling in humans supports not only encoding but also retrieval. They further suggest that hippocampal theta is coupled to gamma oscillations outside the HC proper (i.e. in the PHG). This interpretation, however, should be taken with some caution since we analyzed our data with a bipolar reference scheme and, due to the relatively small sample of MTL electrodes, did not exclude virtual bipolar electrodes that shared a physical electrode. Although unlikely, our results might therefore be based on within-region coupling in HC, PHG, or both. In our data set, PAC did not seem to be related to behavioral clustering or spatial information transfer between HC and PHG (as obtained from our similarity analysis) across subjects. This null result might be due to a lack of power or suggest that PAC supports retrieval more generally, i.e. by a mechanism other than conveying spatial information from HC to PHG.

Although we have interpreted our findings as demonstrating the reinstatement of spatial information during the recall phase, it is also possible that spatial clustering arises due to the reactivation of object representations during encoding. Specifically, if subjects reactivate object representations whenever they visit locations close to an object's initial encoding location, this would establish temporal associations between objects encoded in proximate locations – spatial context would become an integral part of temporal context. In the recall phase, temporal context would then be sufficient to cue items from a proximate location. We believe that this process might enhance the observed effects, but it seems unlikely to explain them entirely, as it would mean that spatial context reliably cues items during encoding but completely fails to do so during recall.

Conclusions

Using a hybrid spatial-episodic memory task, we show that episodic memories are organized by spatial study context, resulting in a spatial contiguity effect that parallels the often-reported temporal contiguity effect in free recall. We further demonstrate that increased medial temporal theta power accompanies retrieval of spatial context and associated clustering behavior, implicating theta oscillations as a common neurophysiological substrate of spatial coding in navigation and episodic retrieval. Exploring the temporal dynamics of reinstatement in HC and PHG, we find that spatial context information is initially retrieved in the HC and from there relayed to cortical modules in the PHG, supporting the notion that the predominant direction of information flow in the MTL reverses during retrieval. Finally, we demonstrate that hippocampal theta phase modulates parahippocampal gamma amplitude, suggesting a role for cross frequency coupling in coding and transmitting retrieved information.

Methods

Participants

29 patients with medication-resistant epilepsy undergoing clinical seizure monitoring at Thomas Jefferson University Hospital (Philadelphia, PA, USA), the University Clinic Freiburg (Freiburg, GER) and the Hospital of the University of Pennsylvania (Philadelphia, PA, USA) participated in the study. The study protocol was approved by the Institutional Review Board at each hospital and participants gave written informed consent. Electrophysiological data were recorded from depth electrodes placed, according to clinical considerations, in the HC and/or surrounding PHG.

Experimental design and task

Participants played the role of a courier in a hybrid spatial-episodic memory task, riding a bicycle and delivering parcels to stores located within a virtual town (consisting of roads, stores, task-irrelevant buildings, areas of grass, and props such as fences, streetlights and trees; **Figure 1a-b**). Each experimental session consisted of a series of delivery days (i.e. trials), during which participants navigate to deliver objects and, at the end of each trial, recall those objects. Participants completed slightly different versions of this paradigm, the details of which are described in the following paragraphs. These versions were programmed and displayed to subjects using the Panda Experiment Programming Library [52], which is a Python based wrapper around the open source game engine Panda3d (with 3D models created using Autodesk Maya™) or the

Unity Game Engine (Unity Technologies, San Francisco, CA).

Prior to starting the first delivery day, participants viewed a static or rotating rendering of each store in front of a black background. Each store had a unique storefront and a sign that distinguished it from task-irrelevant buildings. This 'store familiarization' phase was followed by a 'town familiarization' phase, in which participants were instructed to navigate from store to store without delivering parcels (and recalling objects), visiting each store 1-3 times in pseudo-random order (each store was visited once, before the first store was visited the second time). Participants were informed about their upcoming goal by on-screen instructions and navigated using the joystick or buttons on a game pad. Location-store mappings in the town were fixed for 7 participants and random for 22 participants (the layout was always fixed across experimental sessions; i.e. each participant experienced the same town layout across sessions). For a subset of the participants, the town and store familiarization phases were part not only of the first but also all following sessions with just one visit to each store prior to the first delivery day in each session. Furthermore, waypoints helped a subset of participants navigate upon difficulties finding a store. Considering each intersection as a decision point, arrows pointing in the direction of the target store appeared on the street after three bad decisions (i.e. decisions that increased the distance to the target store).

Each delivery day trial consisted of a navigation phase and a free recall phase (and for some participants an additional cued recall phase following free recall, for which no data is reported here; **Figure 1a**). For the navigation phase, 13 stores were chosen at random out of the total number of 16 or 17 stores. Participants navigated to these stores sequentially (including on-screen instructions and waypoints described above). Upon arrival at the first 12 stores, participants were presented with an audio (N = 23 subjects) or an image (N = 6 subjects; 5 s) of the object they just delivered. For some subjects, objects were drawn with and for others without replacement. For 23 participants, objects were semantically related to their target store to aid recall performance. Object presentation was followed by the next on-screen navigation instruction ("Please find store X"). Upon arrival at the final store, where no item was presented, the screen went black and participants heard a beep tone. After the beep, they had 90 s to recall as many objects as they could remember in any order. Vocal responses were recorded and annotated offline. Participants completed a variable number of delivery days per session (min: 2, max: 14, mean = 6). A final free recall phase followed on the last delivery day within each session, for which no data is reported here.

Behavioral analyses of recall transitions

Behavioral data were analyzed using Python version 2.7. To assess organization of recall sequences by retrieved spatial (and temporal) context, we assigned each recall transition the Euclidean (temporal) distance between the two encoding locations (time points). In the same way, we calculated the distance for all possible transitions that could have been made instead of each actual transition (i.e. the distance between the location (time point) of the first item in the transition and all locations (time points) at which objects were encoded that had not yet been recalled at a given recall transition). We then calculated a spatial (temporal) clustering score for each recall transition as the percentile ranking of the spatial (temporal) distance assigned to the actual transition with respect to all possible transitions. The higher the average spatial (temporal) clustering score across recall transitions, the more likely a participant was to transition between items that were encoded at proximate locations (time points). We used a permutation procedure to assess significance of spatial (temporal) clustering across subjects. To do so, all recalled words on a given trial for a given subject were randomly permuted 2000 times. The distribution of average clustering scores across subjects obtained from these random permutations provides a measure of clustering values observed by chance, while controlling for the identity and number of recalled words per trial. The percentage of random clustering scores larger than the observed clustering score constitutes the permutation p-value. To assess the relation between spatial and temporal clustering, we computed the correlation between both variables across subjects.

Intracranial EEG data acquisition and preprocessing

EEG data were acquired using AdTech (Oak Creek, WI, USA), PMT (Chanhassen, MN, USA) or Dixi (Besançon, France) depth electrodes along with a Nihon Koden (Tokyo, Japan), Natus (Pleasanton, CA, USA), Compumedics (Abbotsford, Victoria, Australia) or IT-med (Usingen, Germany) recording system at sampling rates between 400 and 2500 Hz. Coordinates of the radiodense electrode contacts were derived from a post-implant CT or MRI scan and then registered with the pre-implant MRI scan in MNI space using SPM or

Advanced Normalization Tools (ANTS)[53]. EEG data were analyzed using Python version 2.7 along with the Python Time Series Analyses (ptsa; https://github.com/pennmem/ptsa_new) and MNE [54] software packages. EEG data were aligned with behavioral data via pulses send from the behavioral testing laptop to the EEG system. Data were epoched from -1900 ms to 2400 ms with respect to word onset during encoding and from -2750 ms to 2000 ms with respect to recall onset during retrieval periods. Data were re-referenced with a bipolar reference scheme and down-sampled to 400 Hz. A butterworth filter (order 4; cutoff frequencies 48 to 52 for data recorded in Germany and 58 to 62 for data recorded in the US) was used to filter line noise and subsequently outliers were excluded on an epoch by channel basis: The interquartile range (IQR) was calculated for each channel across all (mean-corrected) encoding or retrieval events within a session. Outliers were identified as samples 5 times the IQR above the 75th percentile or 5 times the IQR below the 25th percentile. Epochs were excluded for a given channel with at least one outlying sample. On average 2.5 % (min: 0 %, max 11.0 %) of epoch-channel pairs were excluded per session. To extract power and phase, the data were convolved with complex Morlet wavelets (5 cycles) for 25 log-spaced frequencies between 3 and 100 Hz. After convolution, a buffer was removed at the beginning and end of each epoch leaving a time windows of 100 ms to 400 ms during encoding and -750 ms to 0 ms during recall. Data were z-scored with respect to the mean and standard deviation across all encoding or recall samples within a session and then averaged over time, two frequency bands (theta: 3 to 8 Hz; high gamma: 70 to 100 Hz), and two regions of interest (ROI): HC and PHG as defined by the Harvard Oxford Atlas. Subjects' data were included for a given analysis if they contributed at least 8 valid trials in at least one (or, where necessary, both) ROI(s).

Intracranial EEG data statistical analyses

To assess the spectral correlates of successful spatial context retrieval and associated spatial clustering, we used a within-subject linear regression model. The model relates average theta and high gamma power in the HC (N = 20 subjects) and PHG (N = 19 subjects) preceding recall of the first item in a recall transition to the spatial proximity (i.e. spatial clustering score) associated with that transition. To the extent that retrieved spatial context cues items encoded in close spatial proximity, the spatial proximity of a recall transition should be indicative of spatial context retrieval for the first item in the transition. A β value for spatial proximity above zero indicates increased power during retrieval of spatial context, and a value below zero indicates decreased power during retrieval of spatial context. In addition to the spatial clustering score associated with each recall transition, temporal clustering score, serial position and output position were added as regressors of no interest to account for shared variance with our predictor of interest. The β values for spatial clustering scores per region and frequency band for all subjects were analyzed with a 2×2 ANOVA and a one-sample t-test.

To test for dynamic spatial context reinstatement, time-frequency spectra during encoding and retrieval were concatenated over all electrodes within either HC (N = 20 subjects) or PHG (N = 20 subjects). A single vector representing power for all time-frequency-electrode points within a given ROI during encoding was correlated with a corresponding vector for retrieval derived from a sliding time-window. The sliding time-window equaled the length of the encoding epoch (300 ms) and was centered on every sample (every 2.5 ms) in the retrieval time-window (-750 ms to 0 ms), located at least half a window size (150 ms) from the edges of the retrieval time-window. For each recall event, we calculated the correlation (i.e. neural similarity) with all encoding events on the same list that did not share the same item. We excluded encoding of the respective item to exclude effects driven by reinstatement of item as opposed to context information. We then used a linear regression model relating (Fisher z-transformed) neural similarity at each time point to the spatial proximity (normalized to be between 0 and 1) between the locations of the encoded and recalled item. A β value above 0 indicates higher similarity for encoding-recall pairs that share spatial context and, hence, can be interpreted as reactivated spatial context. Again, we included additional regressors of no interest to account for shared variance: temporal proximity (the negative absolute temporal difference between the two encoding time points) and study-test proximity (the temporal difference between encoding and recall time). We assessed differences across regions at the beginning or the end of the time-series with independent samples t-tests. To quantify the temporal dynamics of reactivated spatial information in HC and PHG, we fitted a regression line to the time series of β parameters in each brain region for each subject. The resulting second-order β parameters describe the temporal trend within

each brain region. We tested for a difference in those parameters using an independent samples t-test across subjects.

To assess theta-phase to gamma-amplitude coupling between HC and PHG (N = 14 subjects), we calculated the SI [40]. This method does not require an a priori assumption about the modulating (low) frequency, but instead this frequency is determined by finding a peak in the power spectrum of the high frequency power envelope. If high frequency power is time-locked to low frequency phase, high frequency power should fluctuate at the lower oscillation frequency. In our analysis we restricted the range of modulating frequencies to the theta band (i.e. 3 to 8 Hz). After determining the modulating frequency for each channel in the PHG, each recall event, and each extracted frequency in the gamma band, we extracted the phase of the high frequency power time series using the Hilbert transform. The SI is then calculated as the consistency across time between the phase of the high frequency power time series and the low frequency filtered signal [40]. The magnitude of the resulting complex number indicates the extent of synchronization and the angle indicates the preferred phase offset. We determined significance using a non-parametric test statistic based on shifting the two phase time series against each other (into the buffer excluded for other analyses) 2000 times to obtain a distribution of SI values as they would be observed based on random phase relationships. We averaged across frequencies in the high gamma band, and then compared the magnitude of the SI of a single electrode pair to its respective random distribution. The percentile ranking of the observed SI within that distribution provides a p-value per electrode. Likewise, comparing the magnitude of the average SI across subjects to the average random distribution provides a p-value at the subject level. These comparisons address slightly different null hypotheses: While significance at the electrode level allows for different phase offsets across electrodes, significance at the subject level relies on similar phase offsets across electrode pairs and subjects. Finally, we asked if PAC was a function of spatial clustering or spatial information transfer. To this end, we correlated (Fisher z-transformed) PAC with spatial clustering scores and the difference in our second-order β parameters describing the temporal trend of spatial information in HC and PHG.

Author contributions

NAH and MJK designed research, NAH analyzed data and drafted the paper, NAH and MJK edited the paper, AB and NAH collected data, AS-B, MS, ADS recruited participants and performed clinical duties associated with data collection including neurosurgical procedures or patient monitoring, MJK supervised research, all authors approved the final version of the paper.

Acknowledgements

This work was supported by NIH grant MH061975 to MJK. We thank Christoph Weidemann for help with data analyses, Paul Wanda, Alison Xu, Zeinab Helili, Katherine Hurley, Deb Levy, Logan O'Sullivan, Ada Aka and Allison Kadel for help with data acquisition and post-processing, Jonathan Miller and Ansh Johri for their contributions to the task design, Corey Novich and Ansh Patel for programming the Unity based experiment, as well as Joel Stein, Rick Gorniak and Sandy Das for electrode localization support. We are most grateful to all patients and their families who selflessly volunteered their time to participate in this research.

References

1. Kahana, M. J. Associative retrieval processes in free recall. *Mem. Cognit.* **24,** 103–109 (1996).
2. Sederberg, P. B., Howard, M. W. & Kahana, M. J. A context-based theory of recency and contiguity in free recall. **115,** 893–912 (2009).
3. Buschman, T. J. & Miller, E. K. Top-down versus bottom-up control of attention in the prefrontal and posterior parietal cortices. *Science (80-.).* **315,** 1860–2 (2007).
4. Ekstrom, A. D. *et al.* Cellular networks underlying human spatial navigation. *Nature* **425,** 184–187 (2003).
5. O'Keefe, J. A review of the hippocampal place cells. *Prog. Neurobiol.* **13,** 419–439 (1979).
6. Jacobs, J. *et al.* Direct recordings of grid-like neuronal activity in human spatial navigation. *Nat. Neurosci.* **16,** 1188–1191 (2013).
7. Hafting, T., Fyhn, M., Molden, S., Moser, M.-B. & Moser, E. I. Microstructure of a spatial map in the entorhinal cortex. *Nature* **436,** 801–806 (2005).
8. Buzsáki, G., Leung, L.-W. S. & Vanderwolf, C. H. Cellular Bases of Hippocampal EEG in the Behaving Rat. *Brain Res. Rev.* **6,** 139–171 (1983).
9. Vanderwolf, C. H. Hippocampal electrical activity and voluntary movement in the rat. *Electroencephalogr. Clin. Neurophysiol.* **26,** 407–418 (1969).
10. Cornwell, B. R., Johnson, L. L., Holroyd, T., Carver, F. W. & Grillon, C. Human Hippocampal and Parahippocampal Theta during Goal-Directed Spatial Navigation Predicts Performance on a Virtual Morris Water Maze. *J. Neurosci.* **28,** 5983–5990 (2008).
11. Bohbot, V. D., Copara, M. S., Gotman, J. & Ekstrom, A. D. Low-frequency theta oscillations in the human hippocampus during real-world and virtual navigation. *Nat. Commun.* **8,** 1–7 (2017).
12. Bush, D. *et al.* Human hippocampal theta power indicates movement onset and distance travelled. *Proc. Natl. Acad. Sci.* **114,** 12297–12302 (2017).
13. Kaplan, R. *et al.* Movement-Related Theta Rhythm in Humans: Coordinating Self-Directed Hippocampal Learning. *PLoS Biol.* **10,** e1001267 (2012).
14. Ekstrom, A. D. *et al.* Human Hippocampal Theta Activity During Virtual Navigation. *Hippocampus* **15,** 881–889 (2005).
15. Aghajan, Z. M. *et al.* Theta Oscillations in the Human Medial Temporal Lobe during Real-World Ambulatory Movement. *Curr. Biol.* **27,** 3743–3751.e3 (2017).
16. Miller, J. F. *et al.* Lateralized hippocampal oscillations underlie distinct aspects of human spatial memory and navigation. *Nat. Commun.* **9,** 2423 (2018).
17. O'Keefe, J. & Recce, M. L. Phase Relationship Between Hippocampal Place Units and the EEG Theta Rhythm. *Hippocampus* **3,** 317–330 (1993).
18. Koenig, J., Linder, A. N., Leutgeb, J. K. & Leutgeb, S. The spatial periodicity of grid cells is not sustained during reduced theta oscillations. *Science (80-.).* **332,** 592–595 (2011).
19. Brandon, M. P. *et al.* Reduction of theta rhythm dissociates grid cell spatial periodicity from directional tuning. *Science (80-.).* **332,** 595–600 (2011).
20. Herweg, N. A. & Kahana, M. J. Spatial representations in the human brain. *Front. Hum. Neurosci.* **12,** 297 (2018).
21. Squire, L. R. & Zola-Morgan, S. The Medial Temporal Lobe Memory System. *Science (80-.).* **253,** 1380–1386 (1991).
22. Mayes, A. R., Montaldi, D. & Migo, E. Associative memory and the medial temporal lobes. *Trends Cogn. Sci.* **11,** 126–135 (2007).
23. Eichenbaum, H., Yonelinas, A. P. & Ranganath, C. The medial temporal lobe and recognition memory. *Annu. Rev. Neurosci.* **30,** 123–152 (2007).
24. Diana, R. A., Yonelinas, A. P. & Ranganath, C. Imaging recollection and familiarity in the medial temporal lobe: A three-component model. *Trends Cogn. Sci.* **11,** 379–386 (2007).
25. Wixted, J. T. & Squire, L. R. The medial temporal lobe and the attributes of memory. *Trends Cogn. Sci.* **15,** 210–217 (2011).
26. Buzsáki, G. Theta rhythm of navigation: Link between path integration and landmark navigation, episodic and semantic memory. *Hippocampus* **15,** 827–840 (2005).
27. Solomon, E. A. *et al.* Functional wiring of the human medial temporal lobe. *bioRxiv* **257899,** (2018).
28. Burke, J. F. *et al.* Theta and High-Frequency Activity Mark Spontaneous Recall of Episodic Memories. *J. Neurosci.* **34,** 11355–11365 (2014).
29. Lega, B. C., Jacobs, J. & Kahana, M. J. Human hippocampal theta oscillations and the formation of episodic memories. *Hippocampus* **22,** 748–761 (2012).
30. Herweg, N. A. *et al.* Theta-alpha oscillations bind the hippocampus, prefrontal cortex, and striatum during recollection: Evidence from simultaneous EEG–fMRI. *J. Neurosci.* **36,** 3579–3587 (2016).
31. Guderian, S. & Düzel, E. Induced theta oscillations mediate large-scale synchrony with mediotemporal areas during recollection in humans. *Hippocampus* **15,** 901–912 (2005).
32. Miller, J. F. *et al.* Neural acitivity in human hippocampal formation reveals the spatial context of retrieved memories. *Science (80-.).* **365,** 1111–1114 (2013).
33. Treves, A. & Rolls, E. T. Computational analysis of the role of the hippocampus in memory.

Hippocampus **4,** 374–391 (1994).

34. Solomon, E. A. *et al.* Widespread theta synchrony and high-frequency desynchronization underlies enhanced cognition. *Nat. Commun.* **8,** (2017).
35. Senior, T. J., Huxter, J. R., Allen, K., O'Neill, J. & Csicsvari, J. Gamma Oscillatory Firing Reveals Distinct Populations of Pyramidal Cells in the CA1 Region of the Hippocampus. *J. Neurosci.* **28,** 2274–2286 (2008).
36. Skaggs, W. E., McNaughton, B. L., Wilson, M. A. & Barnes, C. A. Theta phase precession in hippocampal neuronal populations and the compression of temporal sequences. *Hippocampus* **6,** 149–172 (1996).
37. Dragoi, G. & Buzsáki, G. Temporal Encoding of Place Sequences by Hippocampal Cell Assemblies. *Neuron* **50,** 145–157 (2006).
38. Lisman, J. E. & Jensen, O. The Theta-Gamma Neural Code. *Neuron* **77,** 1002–1016 (2013).
39. Fries, P. A mechanism for cognitive dynamics: Neuronal communication through neuronal coherence. *Trends Cogn. Sci.* **9,** 474–480 (2005).
40. Cohen, M. X. Assessing transient cross-frequency coupling in EEG data. *J. Neurosci. Methods* **168,** 494–499 (2008).
41. Miller, J. F., Lazarus, E. M., Polyn, S. M. & Kahana, M. J. Spatial clustering during memory search. *J. Exp. Psychol. Learn. Mem. Cogn.* **39,** 773–781 (2013).
42. Gmeindl, L., Walsh, M. & Courtney, S. M. Binding serial order to representations in working memory: A spatial/verbal dissociation. *Mem. Cogn.* **39,** 37–46 (2011).
43. Vass, L. K. *et al.* Oscillations Go the Distance: Low-Frequency Human Hippocampal Oscillations Code Spatial Distance in the Absence of Sensory Cues during Teleportation. *Neuron* **89,** 1180–1186 (2016).
44. Staresina, B. P., Cooper, E. & Henson, R. N. A. Reversible information flow across the medial temporal lobe: The hippocampus links cortical modules during memory retrieval. *J. Neurosci.* **33,** 14184–14192 (2013).
45. Moser, E. I., Kropff, E. & Moser, M.-B. Place cells, grid cells, and the brain's spatial representation system. *Annu. Rev. Neurosci.* **31,** 69–89 (2008).
46. Nadasdy, Z. *et al.* Context-dependent spatially periodic activity in the human entorhinal cortex. *Proc. Natl. Acad. Sci.* **114,** E3516–E3525 (2017).
47. Lega, B., Burke, J. F., Jacobs, J. & Kahana, M. J. Slow-Theta-to-Gamma Phase – Amplitude Coupling in Human Hippocampus Supports the Formation of New Episodic Memories. *Cereb. Cortex* **26,** 268–278 (2014).
48. Mormann, F. *et al.* Phase/amplitude reset and theta-gamma interaction in the human medial temporal lobe during a continuous word recognition memory task. *Hippocampus* **15,** 890–900 (2005).
49. Friese, U. *et al.* Successful memory encoding is associated with increased cross-frequency coupling between frontal theta and posterior gamma oscillations in human scalp-recorded EEG. *Neuroimage* **66,** 642–647 (2013).
50. Tort, A. B. L., Komorowski, R. W., Manns, J. R., Kopell, N. J. & Eichenbaum, H. Theta-gamma coupling increases during the learning of item-context associations. *Proc. Natl. Acad. Sci.* **106,** 20942–20947 (2009).
51. Igarashi, K. M., Lu, L., Colgin, L. L., Moser, M. B. & Moser, E. I. Coordination of entorhinal-hippocampal ensemble activity during associative learning. *Nature* **510,** 143–147 (2014).
52. Solway, A., Miller, J. F. & Kahana, M. J. PandaEPL: A library for programming spatial navigation experiments. *Behav. Res. Methods* **45,** 1293–1312 (2013).
53. Avants, B. B., Epstein, C. L., Grossman, M. & Gee, J. C. Symmetric diffeomorphic image registration with cross-correlation: Evaluating automated labeling of elderly and neurodegenerative brain. *Med. Image Anal.* **12,** 26–41 (2008).
54. Gramfort, A. *et al.* MNE software for processing MEG and EEG data. *Neuroimage* **86,** 446–460 (2014).